

Experimental Investigation of Infill Parameters Influence on Compressive Strength-to-Mass Ratio of PLA 3D Printed Part

The Jaya Suteja*

Department of Mechanical and Manufacturing Engineering,
University of Surabaya, Surabaya, INDONESIA
*jayasuteja@staff.ubaya.ac.id

ABSTRACT

An infill pattern can be implemented in manufacturing a porous component using 3D Printing technology to reduce the mass of the printed part. The use of an infill pattern and infill angle affects the structure of the printed part. This research aims to investigate the effect of various infill patterns and angles on the compressive strength-to-mass ratio of components manufactured by 3D Printing. This research implements a General Linear Model analysis with two replications. Seventy-two compressive test specimens, according to ASTM D695, are printed and tested for compression. The experiment results show that the type of infill pattern has a significant effect on the mass. However, the mass is not significantly influenced by the infill angle. In addition, the infill pattern type and the infill angle significantly influence the compressive strength of the specimen. Then, the compressive strength-to-mass ratio is significantly affected by the infill patterns and angles. The results indicate that a part using the Honeycomb infill pattern type gains the highest compressive strength-to-mass ratio compared to other infill patterns. On the opposite, the infill pattern that creates the lowest compressive strength-to-mass ratio compared to other infill patterns is the Archimedean chords type. The use of a 45° infill angle causes the lowest compressive strength-to-mass ratio compared to other infill angles. Using a 90° infill angle causes the highest compressive strength-to-mass ratio compared to other infill angles.

Keywords: *Infill Pattern; Infill Angle; Compressive Strength-to-Mass Ratio; PLA; 3D Printing*

Introduction

3D Printing technology can be used to manufacture various customized components. Some components must have a particular compressive strength value to perform their functions. The compressive strength of a component printed using 3D Printing technology is influenced by various process parameters. Zu et al. [1] investigated the effect of coating thickness, fill density, and printing speed on the compressive strength of components made of PLA material. The results of this study indicate that the layer thickness and filling density have a very significant effect on compressive strength. Cláudio et al. [2] stated that layer thickness is critical in determining compressive strength. The research results of Dave et al. show that the filling density significantly influences compressive strength [3]. Very similar results are also observed in the study by Abbas et al. [4], Chen et al. [5], and Waseem et al. [6]. Meanwhile, Singh et al. [7] state similar results for different materials.

In addition, Huu et al. [8] investigated the effect of layer thickness and build orientation on compressive strength. From the results of this study, layer thickness and build orientation significantly influence compressive strength. Maszybrocka et al. [9] found that the outer layers of the printed part influence the compressive strength of the part. Research conducted by Balamurugan et al. [10] added that the bed and nozzle temperature also affect the compressive strength of a 3D-printed part. The study by Alfonso et al. [11] also indicated that the nozzle temperature significantly influences the compressive strength of the printed part.

The compressive strength is also affected by the post-processing, such as the heat treatment process, carried out on the printed parts of the 3D Printing process. The research by Hong et al. [12] is conducted to strengthen the properties of the moulded PLA material by heat treatment. The results of this study indicate that heat treatment at a temperature of 130 °C and a holding time of 300 seconds can produce the maximum bending strength of the moulded part. Meanwhile, the compressive strength of the moulded part can reach the highest value by heating at a temperature of 140 °C and holding time for 600 seconds. However, if the temperature and holding time are increased continuously, there is an indication that the compressive strength will also increase.

Aloyaydi et al. [13] stated that the infill pattern used to print the printed part influences the compressive strength of the printed part. An infill pattern is a filling pattern on the inside of a part printed with 3D Printing. Aloyaydi's research uses four infill patterns: triangle, grid, quarter cubic, and tri-hexagon [13]. Based on the study, the cubic type parts showed the highest compressive strength values. The research conducted by Yadav et al. [14] investigated the effect of six types of infill patterns, which are Hilbert curve, honeycomb, line, rectilinear, Archimedean curve, and octagram spiral, on compressive strength. Among these six types of infill patterns, the Hilbert curve type results in the

most significant compressive strength value. Kona et al. [15] found that the honeycomb type of infill pattern builds a higher compressive strength structure than the wiggle, triangle, and rectilinear types. Parab and Zaveri [16] also investigated the effect of three infill pattern types, line, triangle, and gyroid, on compressive strength. The results of this study indicate that the triangle type can produce parts with better compressive strength than the other two infill pattern types. However, the gyroid type will produce components with almost isotropic properties and have similar compressive strengths when subjected to compressive loads from any direction. This finding is also supported by research conducted by Silva et al. [17].

Based on research by Khan et al. [18], the compressive strength of the printed part is also affected by the raster or infill angle. This study uses three infill angles, which are 0° , 45° , and 60° . The study by Kain et al. [19] also shows a direct interaction between the infill angle and the resulting compressive strength. This study investigated the effect of seven kinds of infill angles on the compressive strength of the printed part, which are 0° , 15° , 30° , 45° , 60° , 75° , and 90° .

The infill pattern can be implemented to manufacture a porous component to reduce the volume and mass of the printed part. Using this infill pattern also causes the printed part to have a different compressive strength. According to Suteja [20], five other infill patterns can be used in the 3D printing process, which are 3D honeycomb, stars, cubic, concentric, and grid. As the infill angle affects the compressive strength of the printed part, the influence of a combination of the types of infill patterns and the infill angles on the compressive strength needs to be studied. The mass of the part that is printed using the combination of various types of infill patterns and the infill angles also needs to be investigated as the required material mass affects the cost of the part. Therefore, it is necessary to examine the influence of various infill patterns and angles on compressive strength and mass to produce a component with a high compressive strength-to-mass ratio.

This research aims to investigate the effect of various infill patterns and angles on the compressive strength and the mass of parts manufactured by 3D printing. The compressive strength value is then divided by the mass of the required material. This compressive strength-to-mass ratio indicates the combination of various infill patterns and angles that can be used to manufacture printed parts with high compressive strength and low required material mass. By knowing the compressive strength-to-mass ratio, the feasibility of 3D printing technology in manufacturing various customized components can be analysed further.

Research Methodology

The 3D printer utilized in this research is the ANET A8 Prusa I3. The 3D printer implements Fused Filament Fabrication (FFF) type technology. The printing area of the 3D printer is 220 x 220 x 240 mm. The extruder of the 3D printer has a nozzle diameter of 0.4 mm. This 3D printer is used to heat CCTREE Polylactic Acid (PLA) material to a temperature of 210 °C. The PLA material used in this study is initially a filament with a diameter of 1.75 mm. The PLA material is used because it is an environmentally friendly material and is easy to obtain but has low strength compared to other FFF materials. After softening, the filament is extruded to exit through the nozzle at a certain speed so that it has the same diameter as the nozzle diameter. The filaments are printed layer by layer and raster by raster on a heated bed to produce parts designed to resemble ASTM D695 specimens [21]. The shape and size of this test specimen can be seen in Figure 1. Previously, the bed was preheated until it reached a temperature of 65 °C. The path of the printed filament is generated based on the chosen infill pattern type. As all the infill pattern types mentioned by Suteja [20] are widely used, this research investigates all infill pattern types shown in Figure 2 as research factors. Meanwhile, only three infill angles, 0°, 45°, and 90° are explored in this research. These three infill angles are selected to represent the influence of the infill angles to reduce the investigation time and effort.

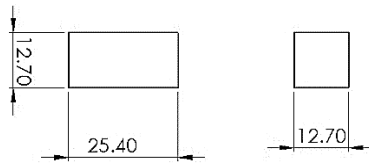


Figure 1: Shape and size of the ASTM D695 specimen in millimeters

To generate the path of the printed filament, this study used Prusa's Slic3r embedded in Repetier-Host software developed by Hot-World GmbH & Co. KG. This software is also used to set the 3D printing process parameters. In this research, the infill density used was 50% to make the effect of the infill pattern on the compressive strength visible. Figure 3 shows the printed infill pattern types investigated in this research. The test specimen is printed parallel to the X-Y or flat surface, as shown in Figure 4(a). The raster angle forms an angle of 0°, 45°, and 90° to the X-axis, as shown in Figure 4(b). In the compression testing, the printed specimen bears the compressive load applied perpendicular to the X-Z surface, as shown in Figure 4(c). The independent process parameters used in this research are shown in Table 1.

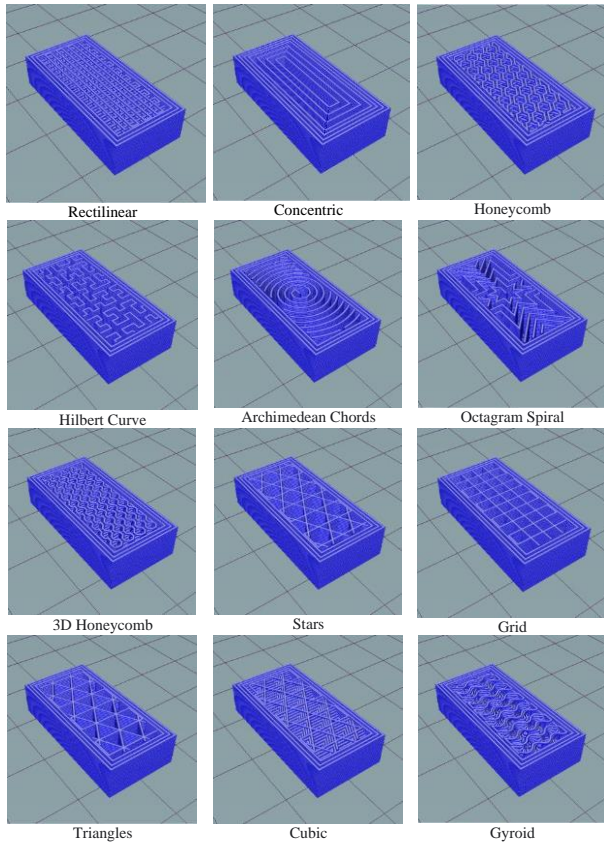


Figure 2: Investigated infill pattern types

As the experiment involves a general linear model analysis, thirty-six test specimens were printed using different infill patterns and angles. The printing of these specimens was carried out in two replications. Because this study aims to study the compressive strength of the printed part using various types of infill patterns and infill angles, a total of seventy-two specimens that have been printed are then tested for compression using the Universal Testing Machine produced by GOTECH Testing Machines Inc. Before the compression test, the cross-sectional dimensions of the seventy-two specimens were measured using a caliper with an accuracy of 0.01 mm. After that, each specimen's material mass is measured using Denver Instrument Company AA-200 with 0.0001-gram accuracy. The compressive strength can be calculated by dividing the compressive force obtained from the Universal Testing Machine by the cross-sectional area of each specimen.



Rectilinear



Concentric



Honeycomb



Hilbert Curve



Archimedean Chords



Octagram Spiral



3D Honeycomb



Stars



Grid



Triangle



Cubic



Gyroid

Figure 3: Printed infill pattern types

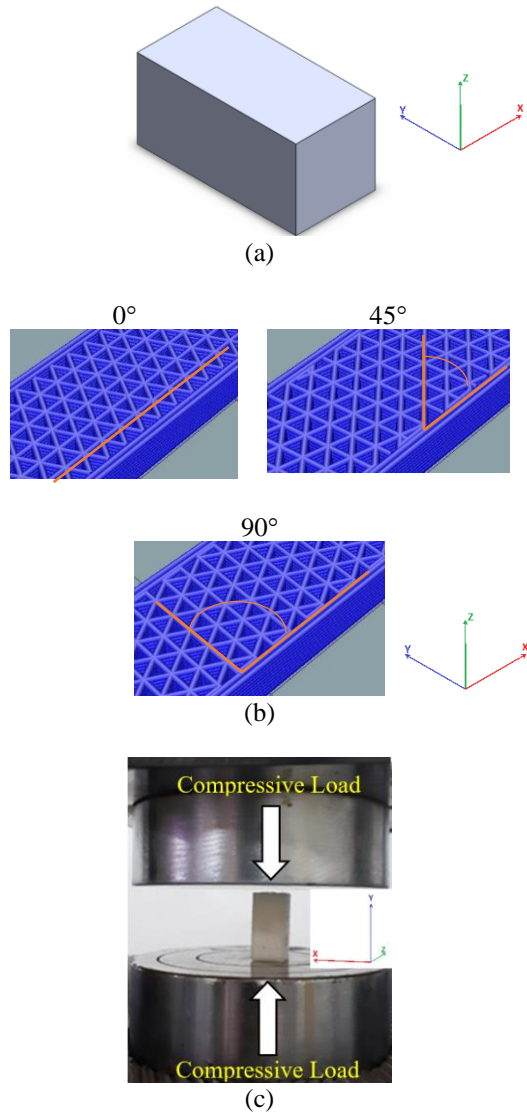


Figure 4: (a) Printing coordinate, (b) infill angle determination, and (c) compressive load coordinate

Table 1: Independent process parameter

Parameters	Value
Nozzle diameter (mm)	0.4
Bed temperature (°C)	65
Nozzle temperature (°C)	210
Printing rate (mm/s)	40
Layer thickness (mm)	0.3
Number of shells	2
Infill density (%)	50
Build orientation	X-Y

Results and Discussion

Table 2 shows the mass of specimens using various types of infill patterns and angles. According to Table 2, the infill pattern type significantly affects the mass. However, the mass is not significantly influenced by the infill angle. Analysis of Variance (ANOVA) for mass performed at a 95% confidence level and significance level $\alpha = 0.05$, as shown in Table 3, exhibits that the p -value of the infill pattern is 0.00 and the p -value of the infill angle is 0.29. Therefore, the result shows the infill pattern type significantly affects the mass, but the infill angle does not. Previous research shows that each infill pattern type requires a different material length to print the infill pattern [20]. The required filament length influences the mass of the specimen. Meanwhile, the infill angle does not affect the required length of the filament material. Therefore, the infill pattern has the most influence on the mass of the specimen. According to Prusa's Slic3r, the longest filament material length is required by the honeycomb type with a 0° infill angle. In contrast, the Gyroid type with a 45° infill angle requires the shortest filament material. Based on the experiment results, the largest and smallest masses are achieved using a honeycomb infill pattern with a 0° infill angle and a Gyroid infill pattern with a 45° infill angle, respectively. The experiment result is in accordance with the required filament length calculated by Prusa's Slic3r and the previous research.

The compressive strength of the specimens using various infill pattern types is shown in Table 4. The table shows a significant relationship between the infill pattern type and the compressive strength of the specimen. The infill angle also has a significant influence on compressive strength. It is in accordance with the ANOVA result performed at a 95% confidence level and significance level $\alpha = 0.05$, shown in Table 5. Both the p -value of the infill pattern and the infill angle are 0.00. Therefore, the result shows the infill pattern type and infill angle significantly affect the compressive strength. The load distribution to each structure member and the cross-section area of the structural member influence the compressive strength of a structure. The infill

pattern and infill angle of the specimen affect the load distribution. The structure member of a different specimen with different infill patterns and angles can bear different loads. As a result, each specimen printed with a different infill pattern and angle has different compression strength. The compressive strength test results show that the specimen using a honeycomb infill pattern with a 0° infill angle can bear the highest compressive load. In contrast, the Archimedean chords type with a 45° infill angle can hold the lowest compressive load. As visualised in Figure 2, the honeycomb infill pattern effectively distributes the compressive load to each structure member [22]. As a result, each structure member bears the lowest load compared to other combinations of infill patterns and angles. Meanwhile, the Archimedean chords type does not distribute the load to its structure members. As a result, the structure's perimeter bears a higher load than other infill patterns and angles. The results also show that the use of different infill angles for a specific infill pattern causes different compressive strengths. On average, the specimen printed using a 45° infill angle has a lower compressive strength than other infill angles. The reason is that different infill angle also causes a significant difference in load distribution, as shown in Figure 5. The results are consistent with the findings of the research by Pernet et al. [23] and Cabreira et al. [24]. The patterns that are aligned with the axes of the load can handle the load, similar to a column, and prevent structure deformation.

Table 2: Experiment result of mass

Infill pattern	Mass (gram)		
	Infill angle 0°	Infill angle 45°	Infill angle 90°
3D honeycomb	3.4402	3.3106	3.4044
Archimedean chords	3.0575	3.0475	3.0714
Concentric	3.2374	3.2304	3.2468
Cubic	3.2182	3.2645	3.2409
Grid	3.2431	3.2806	3.1515
Gyroid	2.7998	2.7861	2.8016
Hilbert curve	3.0290	3.1087	3.0291
Honeycomb	3.5403	3.5178	3.5252
Octagram spiral	3.0984	3.1033	3.0988
Rectilinear	3.1821	3.2935	3.1639
Stars	3.1782	3.2502	3.2566
Triangles	3.1857	3.2595	3.2657

Table 3: Analysis of variance for mass

Source	DF	Seq SS	Adj SS	Adj MS	F	P
Infill pattern	11	216.703	216.703	0.19700	89.59	0.000
Infill angle	2	0.00555	0.00555	0.00277	1.26	0.291
Error	58	0.12753	0.12753	0.00220		
Total	71	2.30011				
S = 0.0468921		R-Sq = 94.46%		R-Sq(adj) = 93.21%		

Table 4: Experiment result of compression strength

Infill Pattern	Compression strength (MPa)		
	Infill angle	Infill angle	Infill angle
	0°	45°	90°
3D honeycomb	21.90	21.20	23.50
Archimedean chords	10.10	8.20	10.00
Concentric	15.65	10.45	16.30
Cubic	20.45	18.95	21.40
Grid	20.05	13.75	20.90
Gyroid	15.85	16.65	16.75
Hilbert curve	10.90	9.85	10.45
Honeycomb	24.60	23.50	22.10
Octagram spiral	11.40	9.80	11.45
Rectilinear	11.00	14.05	19.80
Stars	15.25	16.75	19.45
Triangles	13.75	13.50	18.90

Table 5: Analysis of variance for compression strength

Source	DF	Seq SS	Adj SS	Adj MS	F	P
Infill pattern	11	1340.74	1340.74	121.89	23.86	0.000
Infill angle	2	99.28	99.28	49.64	9.72	0.000
Error	58	296.25	296.25	5.11		
Total	71	1736.27				
S = 2.26004		R-Sq = 82.94%		R-Sq(adj) = 79.11%		

Table 6 shows the compressive strength-to-mass ratio of various infill patterns and angle combinations. As shown in Table 6, the compressive strength-to-mass ratio is influenced by the infill patterns and angles. It is in accordance with the result of the ANOVA performed at a 95% confidence level and significance level $\alpha = 0.05$ that shows both the p -value of the infill pattern and the infill angle is 0.00. The ANOVA result is shown in Table 7. The use of a 45° filling angle results in the lowest compression force-mass ratio

compared to other filling angles. The highest compressive strength-mass ratio is achieved by applying a 90° filling angle. The Archimedean chords type with a 45° infill angle has the lowest compressive strength-to-mass ratio. The highest ratio is obtained using the Honeycomb type with a 0° infill angle. The highest compressive strength to mass ratio represents the type of infill pattern that produces a component with equal compressive strength but requires the least material or shows the infill pattern type that produces the highest compressive strength component using the same amount of material.

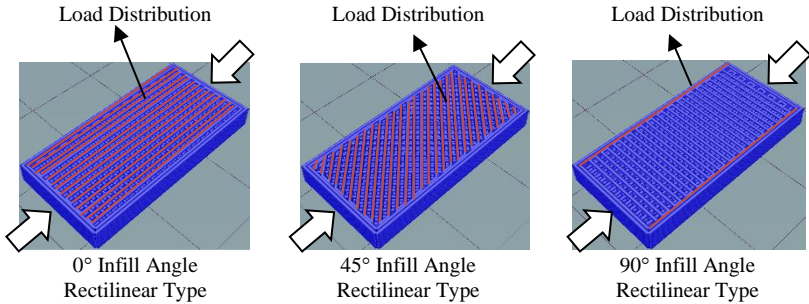


Figure 5: Differences in load distribution

Table 6: Experiment result of compression strength-to-mass ratio

Infill pattern	Compression strength-to-mass ratio (MPa/gram)		
	Infill angle	Infill angle	Infill angle
	0	45	90
3D honeycomb	6.3547	6.4038	6.9093
Archimedean chords	3.3029	2.6897	3.2567
Concentric	4.8342	3.2345	5.0207
Cubic	6.3555	5.8081	6.6036
Grid	6.1817	4.1910	6.6318
Gyroid	5.6568	5.9757	5.9794
Hilbert curve	3.5983	3.1689	3.4499
Honeycomb	6.9486	6.6804	6.2681
Octagram spiral	3.6791	3.1586	3.6977
Rectilinear	3.4578	4.2631	6.2608
Stars	4.7983	5.1537	5.9723
Triangles	4.3162	4.1418	5.7888

Table 7: Analysis of variance for compression strength-to-mass ratio

Source	DF	Seq SS	Adj SS	Adj SS	F	P
Infill pattern	11	100.8571	100.8571	9.1688	18.10	0.000
Infill angle	2	10.3300	10.3300	5.1650	10.20	0.000
Error	58	29.3817	29.3817	0.5066		
Total	71	140.5688				
S = 0.711745		R-Sq = 79.10%		R-Sq(adj) = 74.41%		

Conclusions

The infill pattern type influences the compressive strength and the mass of material required to print the 3D printing part. The infill angle affects only the compressive strength of the printed part. Both the infill pattern type and the infill angle have a significant influence on the compressive strength-to-mass ratio. The part using the Honeycomb infill pattern type obtains the highest compressive strength-to-mass ratio compared to other infill patterns. On the opposite, the infill pattern that creates the lowest compressive strength-to-mass ratio compared to other infill patterns is the Archimedean chords type. Using a 45° infill angle causes the lowest compressive strength-to-mass ratio compared to other infill angles. The highest compressive strength-to-mass ratio is obtained by implementing a 90° infill angle. Although the honeycomb infill pattern type with a 0° infill angle produces a specimen with the highest mass value, it creates the highest compressive strength specimen. Therefore, the Honeycomb infill pattern type with a 0° infill angle is the optimum option because it can be implemented to print a component that can hold a large compressive strength with less material. For future work, the research is extended to investigate the influence of the infill parameters on the other mechanical properties of the PLA 3D printed part.

Contributions of Authors

The author confirms that this work is individual. The author reviewed and approved the final version of this work.

Funding

This work received no specific grant from any funding agency.

Conflict of Interests

The author declares that they have no conflicts of interest

Acknowledgment

The author would like to express our gratitude to the Product Design and Manufacturing Research Groups of the University of Surabaya for providing some resources for the experiment.

References

- [1] Z. Yu, Y. Chao, J. Jiang, H. Gu, S. Lv, H. Ni, X. Wang, and C. Jia, "Study on effects of FDM 3D printing parameters on mechanical properties of polylactic acid," *IOP Conference Series: Materials Science and Engineering*, vol. 688, no. 3, pp. 0–5, 2019.
- [2] R. A. Cláudio, J. Dupont, R. A. Baptista, M. Leite, and L. Reis, "Behaviour evaluation of 3D printed polylactic acid under compression," *Journal of Materials Research and Technology*, vol. 21, pp. 4052-4066, 2022.
- [3] H. K. Dave, S. R. Rakpurohit, N. H. Patadiya, S. J. Dave, K. S. Sharma, S. S. Thambad, V. P. Srinivasn, and K. V. Sheth, "Compressive Strength of PLA based Scaffolds: Effect of layer height, Infill Density and Print Speed," *International Journal of Modern Manufacturing Technologies*, vol. 11, no. 1, pp. 21–27, 2019.
- [4] T. F. Abbas, F. M. Othman, and B. H. Ali, "Effect of infill Parameter on compression property in FDM Process," *International Journal of Engineering Research and Application*, vol. 7, no. 10, pp. 16–19, 2017.
- [5] R. Chen, L. Baich, J. Lauer, D. Senesky, and G. Manogharan, "Effects of part orientation, printer selection, and infill density on mechanical properties and production cost of 3D printed flexural specimens," *Manufacturing Letters*, vol. 33, pp. 549-560, 2020.
- [6] M. Waseem, T. Habib, U. Ghani, M. Abas, Q. M. U. Jan, and M. A. Z. Khan, "Optimisation of tensile and compressive behaviour of PLA 3D printed parts using categorical response surface methodology," *International Journal of Industrial and System Engineering*, vol. 41, no. 4, pp. 417–437, 2022.
- [7] R. Singh, G. Singh, J. Singh, and R. Kumar, "Investigations for tensile, compressive and morphological properties of 3D printed functional prototypes of PLA-PEKK-HAp-CS," *Journal of Thermoplastic of Composite Materials*, vol. 34, no. 10, pp. 1408-1427, 2019.
- [8] N. H. Huu, D. P. Phuoc, T. N. Huu, and H. T. T. Thu, "Optimization of

- the FDM parameters to improve the compressive strength of the pla-copper based products,” *IOP Conference Series: Materials Science and Engineering*, vol. 530, no. 1, pp. 0–10, 2019.
- [9] J. Maszybrocka, M. Dworak, G. Nowakowska, P. Osak, and B. Łosiewicz, “The influence of the gradient infill of pla samples produced with the FDM technique on their mechanical properties,” *Materials*, vol. 15, no. 4, p. 1304, 2022.
- [10] K. Balamurugan, M. Venkata Pavan, S. K. Ahamad Ali, and G. Kalusuraman, “Compression and flexural study on PLA-Cu composite filament using FDM,” *Materials Today: Proceeding*, vol. 44, no. 1, pp. 1687–1691, 2021.
- [11] J. A. Afonso, J. L. Alves, G. Caldas, B. P. Gouveia, and J. Belinha, “Influence of 3D printing process parameters on the mechanical properties and mass of PLA parts and predictive models,” *Rapid Prototyping Journal*, vol. 27, no. 3, pp. 487-495, 2021.
- [12] J. H. Hong, T. Yu, Z. Chen, S. J. Park, and Y. H. Kim, “Improvement of flexural strength and compressive strength by heat treatment of PLA filament for 3D-printing,” *Modern Physics Letters B*, vol. 33, no. 14–15, pp. 3–7, 2019.
- [13] B. Aloyaydi, S. Sivasankaran, and A. Mustafa, “Investigation of infill-patterns on mechanical response of 3D printed poly-lactic-acid,” *Polymer Testing*, vol. 87, p. 1-9, 2020.
- [14] P. Yadav, A. Sahai, and R. S. Sharma, “Strength and surface characteristics of FDM-based 3D printed PLA parts for multiple infill design patterns,” *Journal of The Institution Engineeris (India): Series C*, vol. 102, no. 1, pp. 197–207, 2021.
- [15] S. Kona, K. C. Sekhar, A. Lakshumu Naidu, and V. V Rama Reddy, “Evaluation of compressive strength of thermoplastic materials prepared using 3D printer with different in-fill structures,” in *Advanced Manufacturing Systems and Innovative Product Design*, eds, Springer, Singapore, 2021, pp. 209-215.
- [16] S. Parab and N. Zaveri, “Investigating the influence of infill pattern on the compressive strength of fused deposition modelled PLA parts,” *Proceedings of International Conference on Intelligent Manufacturing and Automation. Lecture Notes Mechanical Engineering*, Springer, Singapore, 2020, pp. 239–247.
- [17] C. Silva, A. I. Pais, G. Caldas, B. P. P. A. Gouveia, J. L. Alves, and J. Belinha, “Study on 3D printing of gyroid-based structures for superior structural behaviour,” *Progress in Additive Manufacturing*, vol. 6, pp. 689-703, 2021.
- [18] S. F. Khan, M. M. Zukhi, H. Zakaria, and M. A. M. Saad, “Optimise 3D printing parameter on the mechanical performance of PLA-wood fused filament fabrication,” *IOP Conference Series: Materials Science and Engineering*, vol. 670, no. 1, pp.1-6, 2019.

- [19] S. Kain, J. V. Ecker, A. Haider, M. Musso, and A. Petutschnigg, "Effects of the infill pattern on mechanical properties of fused layer modeling (FLM) 3D printed wood/polylactic acid (PLA) composites," *European Journal of Wood and Wood Products*, vol. 78, no. 1, pp. 65–74, 2020.
- [20] J. Suteja, "Effect of infill pattern, infill density, and infill angle on the printing time and filament length of 3D Printing," *Jurnal Rekayasa Mesin*, vol. 12, no. 1, p. 145, 2021.
- [21] A. D. 695, "Standard test method for compressive properties of rigid plastics," in ASTM Int. West Conshohocken, PA, USA, 2010.
- [22] M. Moradi, A. Aminzadeh, D. Rahmatabadi, and A. Hakimi, "Experimental investigation on mechanical characterization of 3D printed PLA produced by fused deposition modeling (FDM)," *Materials Research Express*, vol. 8, no. 3, p. 035304, 2021.
- [23] V. Cabreira and R. M. C. Santana, "Effect of infill pattern in Fused Filament Fabrication (FFF) 3D Printing on materials performance," *Materia (Rio de Janeiro)*, vol. 25, no. 3, pp.1-9, 2020.
- [24] B. Pernet, J. K. Nagel, and H. Zhang, "Compressive Strength Assessment of 3D Printing Infill Patterns," *Procedia CIRP*, vol. 105, pp. 682–687, 2022.